Memoirs of the Faculty of Engineering, Nagoya University
Vol.43, No.2 (1991) —Research Report—

NUMERICAL SIMULATION OF REACTIVE FLOWS BY A TIME-SPLIT ALGORITHM

S. G. Ravi KUMAUR and Toshi FUJIWARA

Department of Aeronautical Engineering

(Received October 1, 1991)

Abstract

The propagation of shock-initiated reaction in a two-dimensional channel is studied by a time-split alogrithm. The convection and reaction processes are solved in a decoupled manner. The Euler equation describing the two-dimensional invicid flow is solved by an explicit TVD scheme while the equations describing the reaction kinetics are solved implicitly at each nodal point. The initiation of combustion by a shock wave and its development into a detonation in a $2H_2 + O_2 + 7Ar$ system are studied using the present algorithm. The time history of the process is presented.

1. Introduction

In the last two decades the technique to solve a hyperbolic system of equations describing invicid compressible flows has evolved into high resolution schemes like TVD ones.[1,2,3] The inclusion of chemical reaction processes made the solution procedure complex and time consuming. The wide variations in the time scales of reaction and the propagation of discontinuities imposed constraints on the time step. Implicit methods proved to be stable but time consuming. One such implicit method was applied to the computation of a three-dimensional chemically reacting flow by K. V. Reddy and T. Fujiwara[7] using a shock fitting method. High resolution difference schemes like TVD ones were developed and were successfully applied to fluid-dynamic and combustion problems by Harten,[1] Yee,[2] Osher and Chakravarthy,[3] and others. They were applied to combustion and detonation problems by Yee and Shin,[4] Wang and Fujiwara,[5] respectively. They solved the combustion problems in a coupled manner. On the other hand, E. S. Oran, T. R. Young and J. P. Boris[7] solved the hydrodynamic equations by FCT (Flux Corrected Transport) algorithm and solved the chemical kinetic equations by an asymptotic method.

In the present work described below, the hydrodynamic and reaction parts are solved in a decoupled manner. The hydrodynamic equations are solved explicitly by a TVD scheme while the chemical reaction equations are solved implicitly: The species conservation is strictly imposed in the solution procedure.

2. Outline of solution algorithm

The solution algorithm used in the present simulation is explained in the following steps. The density of each species involved, the momentum and the energy at time t^n are assumed to be known at all the nodal points in the finite difference grid.

(1) The time step $\triangle t^n$ is calculated, based on the values at time t^n and the CFL number.
(2) The hydrodynamic values of the species densities, momentum and energy after the time step $\triangle t^n$ are calculated by an explicit TVD scheme.
(3) The velocities, pressure and temperature are calculated from Step (2) solution.
(4) The time step $\triangle t^n$ is divided into two or more sub-steps and the reaction equations are solved implicitly for each sub-step with input from the previous sub-step. The temperature and pressure are updated after each sub-step.
(5) Conservation of species is checked at each sub-step. If the conservation is not within limits, then the number of sub-steps are increased for the next time step. Normally the hydrodynamic time step is divided into 2 reaction sub-steps.
(6) The temperature and pressure are updated after all the sub-steps.
(7) The calculation is continued to Step (1) for the next time step.

The hydrodynamic solution procedure and the reaction solution procedure are explained in the following sections. The grid adaptation technique and other techniques used to reduce the computational time are also explained.

3. The Governing equations

The system of equations governing the reaction process in an invicid flow can be written as

$$\frac{\partial Q}{\partial t}+\frac{\partial F}{\partial x}+\frac{\partial G}{\partial y}=S, \tag{1}$$

where

$$Q=\begin{bmatrix}\rho_1\\ \rho_2\\ \vdots\\ \rho_n\\ \rho u\\ \rho v\\ e\end{bmatrix},\quad F=\begin{bmatrix}\rho_1 u\\ \rho_2 u\\ \vdots\\ \rho_n u\\ \rho u^2+P\\ \rho uv\\ (e+P)u\end{bmatrix},\quad G=\begin{bmatrix}\rho_1 v\\ \rho_2 v\\ \vdots\\ \rho_n v\\ \rho uv\\ \rho v^2+P\\ (e+P)v\end{bmatrix},\quad S=\begin{bmatrix}\omega_1^*\\ \omega_2^*\\ \vdots\\ \omega_n^*\\ 0\\ 0\\ 0\end{bmatrix}. \tag{2}$$

Let Jacobians A and B be defined as $A=\frac{\partial F}{\partial Q}$, $B=\frac{\partial G}{\partial Q}$.

$$P=\rho R^* T, \tag{3}$$

$$\rho=\sum_{i=1}^{ns}\rho_i, \tag{4}$$

$$R^* = \frac{R_u}{\rho} \sum_{i=1}^{ns} \frac{\rho_i}{M_i}, \tag{5}$$

$$e = \sum_{i=1}^{ns} (\rho_i \cdot h_i) + 0.5\rho(u^2 + v^2) - P. \tag{6}$$

The enthalpy h_i of the species involved in the calculation is evaluated from the polynomial of the form

$$h_i = \sum_{j=1}^{5} b_{ij} (T/1000)^j, \tag{7}$$

which is derived using the values in JANAF Tables. The coefficients in the polynomial are tabulated in Appendix C.

Eq. (1) can be written in a generalised coordinate as

$$\frac{\partial \hat{Q}}{\partial t} + \frac{\partial \hat{F}}{\partial \varepsilon} + \frac{\partial \hat{G}}{\partial \eta} = \hat{S}, \tag{8}$$

where

$$\hat{Q} = J^{-1} Q,$$

$$\hat{F} = J^{-1} (\varepsilon_x F + \varepsilon_y G),$$

$$\hat{G} = J^{-1} (\eta_x F + \eta_y G),$$

$$\hat{S} = J^{-1} S \quad \text{and}$$

J is the Jacobian in the coordinate transformation.
The Jacobians of $\hat{F}$ and $\hat{G}$ can then be written as

$$\hat{A} = \varepsilon_x A + \varepsilon_y B,$$

$$\hat{B} = \eta_x A + \eta_y B.$$

The eigen values of the Jacobians $\hat{A}$ and $\hat{B}$ are given as

$$(a_\varepsilon^1, a_\varepsilon^2, \ldots, a_\varepsilon^{n+3}) = (U, U, \ldots, U + k_\varepsilon a, U, U - k_\varepsilon a),$$

$$(a_\eta^1, a_\eta^2, \ldots, a_\eta^{n+3}) = (V, V, \ldots, V + k_\varepsilon a, V, V - k_\eta a),$$

where

$$U = \varepsilon_x u + \varepsilon_y v,$$

$$V = \eta_x u + \eta_y v,$$

$$k_\varepsilon = \sqrt{\varepsilon_x^2 + \varepsilon_y^2},$$

$$k_\eta = \sqrt{\eta_x^2 + \eta_y^2},$$

and 'a' is the frozen speed of sound;

$$a^2 = P_\rho + P_e(H - u^2 - v^2),$$

$$P_\rho = \sum_{i=1}^{ns} C^i P_{\rho^i},$$

$$P_{\rho^i} = \frac{\partial P}{\partial \rho^i} | m, n, e,$$

$$P_e = \frac{\partial P}{\partial e} | m, n, \rho^1, \ldots, \rho^{ns},$$

$$H = \frac{(e+P)}{\rho}.$$

4. Numerical Modelling

4. 1. Hydrodynamic Calculation

Since the reaction problem is solved in a decoupled manner, the hydrodynamic equations to be solved become

$$\frac{\partial \hat{Q}}{\partial t} + \frac{\partial \hat{F}}{\partial \varepsilon} + \frac{\partial \hat{G}}{\partial \eta} = 0. \tag{9}$$

If the values of $\hat{Q}$ are known at time t^n for the above equations, then the values at time t^{n+1} can be evaluted explicitly by the TVD scheme;[2)]

$$\hat{Q}^{n+1} = \hat{Q}^n - \frac{\triangle t}{\triangle \varepsilon}(\tilde{F}^n_{i+\frac{1}{2},j} - \tilde{F}^n_{i-\frac{1}{2},j}) - \frac{\triangle t}{\triangle \eta}(\tilde{G}^n_{i,j+\frac{1}{2}} - \tilde{G}^n_{i,j-\frac{1}{2}}), \tag{10}$$

where

$$\tilde{F} = \frac{1}{2}(\hat{F}_{i,j} + \hat{F}_{i+1,j} + \frac{R_{i+\frac{1}{2},j}\,\Phi_{i+\frac{1}{2},j}}{J_{i+\frac{1}{2},j}}).$$

$R_{i+\frac{1}{2},j}$ is the eigen matrix for $\hat{A}$.
The element $\phi^l_{i+\frac{1}{2},j}$ of the matrix $\Phi_{i+\frac{1}{2},j}$ for the upwind TVD scheme is

$$\phi^l_{i+\frac{1}{2},j} = \sigma(a^l_{i+\frac{1}{2},j})(g^l_{i+1,j} + g^l_{i,j}) - \phi(a^l_{i+\frac{1}{2},j} + \gamma^l_{i+\frac{1}{2},j})\alpha^l_{i+\frac{1}{2},j}, \tag{12}$$

$$\sigma(z) = \frac{1}{2}[\psi(z) - \frac{\triangle t}{\triangle \varepsilon} z^2], \tag{13}$$

$$\psi(z) = \begin{cases} |z|, & \text{for } |z| \geq \delta_1, \\ \dfrac{(z^2 + \delta^2)}{2\delta}, & \text{for } |z| < \delta_1, \end{cases} \tag{14}$$

$$\alpha^l_{i+\frac{1}{2},j} = R^{-1}_{i+\frac{1}{2},j}(U^l_{i+1,j} - U^l_{i,j}) , \tag{15}$$

$$g^l_{i,j} = minmod(\alpha^l_{i+\frac{1}{2},j} , \alpha^l_{i-\frac{1}{2},j}) , \tag{16}$$

$$\gamma^l_{i+\frac{1}{2},j} = \sigma(\alpha^l_{i+\frac{1}{2},j}) \begin{cases} \dfrac{(g^l_{i+1,j} - g^l_{i,j})}{\alpha^l_{i+\frac{1}{2},j}} , & \text{for } \alpha^l_{i+\frac{1}{2},j} \neq 0 , \\ 0 , & \text{for } \alpha^l_{i+\frac{1}{2},j} = 0 . \end{cases} \tag{17}$$

The average values indicated by the indices $(i+\frac{1}{2}, j)$ are evaluated by Roe's generalised average.[8)]
The time step $\triangle t$ is calculated from

$$\triangle t = CFL/Max(|U| + |V| + a\sqrt{\varepsilon_x^2 + \varepsilon_y^2} + a\sqrt{\eta_x^2 + \eta_y^2}) . \tag{18}$$

δ_1 in Eq. (13) is normally evaluated from the expression

$$\delta_1 = \delta_2(|\tilde{u}| + |\tilde{v}| + \tilde{a})(\varepsilon_x^2 + \varepsilon_y^2)^{\frac{1}{2}} , \tag{19}$$

$$\tilde{u} = \frac{\varepsilon_x u + \varepsilon_y v}{\sqrt{(\varepsilon_x^2 + \varepsilon_y^2)}} , \tag{20}$$

$$\tilde{v} = \frac{\eta_x u + \eta_y v}{\sqrt{(\eta_x^2 + \eta_y^2)}} , \tag{21}$$

$$\tilde{a} = \frac{1}{2} a_{i+\frac{1}{2},j} + \frac{1}{8}(a_{i+\frac{1}{2},j+1} + 2a_{i+\frac{1}{2},j} + a_{i-\frac{1}{2},j-1}) . \tag{22}$$

4. 2. Evaluation of Pressure and Temperature

After each hydrodynamic step calculation the temperature is calculated from Eqs. (3), (6) and (7). Since the values are implicit in the equations, the Newton-Raphson iteration method is used to calculate the temperature and pressure.

4. 3. Chemical Calculation

The chemical process consists of a number of elementary reactions. The production or depletion rate of any species i in a particular elementary reaction r can be written as

$$(\omega_i^*)_r = (\nu''_{ri} - \nu'_{ri}) M_i [k_{fr} \Pi_{j=1}^{ns} C^{\nu''_{ri}} - k_{br} \Pi_{j=1}^{ns} C^{\nu'_{ri}}] . \tag{23}$$

The total production rate of any species from all the elementary reactions can be written as

$$\omega_i^* = \textstyle\sum_{r=1}^{nr} (\omega_i^*)_r . \tag{24}$$

The forward reaction rate constant k_{fr} for an individual reaction is evaluated as

$$k_{fr} = A_r T^{Nr} e^{(-\frac{E_{ar}}{R^* T})} . \tag{25}$$

The backward reaction constant k_{br} is calculated from

$$k_{br} = \frac{k_{fr}}{K_{cr}} . \tag{26}$$

The constants in the forward reation rate equation (25) for the reactions involved in Sample Calculation are given in Appendix A.

The equilibrium constant K_{cr} is evaluated as

$$K_{pr} = K_{cr}(R_o T)^{\triangle \nu} , \tag{27}$$

where

$$\triangle \nu = \sum(\nu_r'' - \nu_r') .$$

The equilibrium pressure constant K_{pr} is calculated by

$$log_{10} K_{pr} = \sum_{j=1}^{ns} (\nu_{jr}'' - \nu_{jr}')(log_{10} K_{pj}) . \tag{28}$$

The value of K_{pi} is evaluated from the polynomial fit

$$log_{10} K_{pi} = \sum_{m=1}^{n} d_{im}(1000/T)^{m-1} . \tag{29}$$

The coefficients d_{im} in the polynomial for the species i involved in Sample Calculation are given in Appendix B.

A set of equations describing the production rate of each species can be written from Eq. (23):

$$\Omega^* = \begin{Bmatrix} \omega_1^* \\ \omega_2^* \\ \vdots \\ \omega_{ns}^* \end{Bmatrix} . \tag{30}$$

The superscript * denotes the production rate of each species at a point in the solution domain. The production rates are the functions of species concentration and temperature. Hence the set Ω^* can be written in a general form as

$$\Omega^* = \hat{\Omega}^*(\omega_1, \omega_2, \ldots, \omega_{ns}, T) . \tag{31}$$

Since the function $\hat{\Omega}^*$ does not depend directly on time, it can be expanded locally around the time t^n as

$$\Omega^* = \Omega^{*n} + \sum_{j=1}^{ns} (\omega_j - \omega_j^n) \frac{\partial \Omega^{*n}}{\partial \omega_j} + (T - T^n) \frac{\partial \Omega^{*n}}{\partial T} . \tag{32}$$

In the system *ns* species exist where the production rate of each species can be written as a function of concentrations and temperature. Finally the energy equation (6) is included into the set.

Then a Jacobian $[A]_r^n$ can be defined as

$$[A]_r^n = \left(\frac{\partial \Omega^{*n}}{\partial \omega_1}, \frac{\partial \Omega^{*n}}{\partial \omega_2}, \ldots, \frac{\partial \Omega^{*n}}{\partial \omega_{ns}}, \frac{\partial \Omega^{*n}}{\partial T} \right). \tag{33}$$

Eq. (32) can be rewritten using the Jacobian $[A]_r^n$ as

$$\Omega^* = \Omega^{*n} + [A]_r^n (\Omega - \Omega^n) + o(h^2). \tag{34}$$

The superscript 'n' refers to the values at time t^n.

To obtain the solution at time t^{n+1}, when the values at a time t^n are given, the modified Euler implicit method[10] can be written as

$$\Omega = \Omega^n + \frac{1}{2} \triangle t(\Omega^* + \Omega^{*n}), \tag{35}$$

where Ω and Ω^* represent the functional values and its derivatives, respectively, at the time t^{n+1}.

Substituting the derivative Ω^* by Eq. (34), Eq. (35) can be written as

$$[I - \frac{\triangle t}{2}[A]_r^n](\Omega - \Omega^n) = \triangle t \Omega^{*n}, \tag{36}$$

where $[I]$ represents the unit matrix.

The system of 'ns + 1' equations can be solved easily by Gauss elimination or matrix inversion. The Jacobian matrix $[A]_r^n$ and the right-hand side term Ω^{*n} of Eq. (36) are evaluated from the values at the time t^n.

Thus in the solution procedure the concentrations and temperature are calculated implicitly. Since the temperature is updated by the implicit solution, the pressure is calculated from the equation of state (3). The partial derivative appearing in the calculation is obtained by the method described in the report on CHEMKIN package.[11]

5. Sample calculation on $2H_2 + O_2 + 7Ar$ system

The algorithm presented above was tested on the $2H_2 + O_2 + 7Ar$ system in a two-dimensional channel. Instead of placing a plane shock wave at the entrance of the channel and allowing it to propagate into the chemical system to ignite and develop into a detonation, a shock wave was automatically created as in a shock tube experiment. The high pressure H_2 is placed at one end, seperating it from the chemical system by an imaginary diaphragm. At the time t=0 the diaphragm is removed. As in a shock tube experiment, a shock wave develops and propagates into the $2H_2 + O_2 + 7Ar$ system. The high temperature behind the shock front initiates combustion, which develops into a shock wave coupled with

combustion. The transient result of one such experiment is presented below. The initial conditions of the numerical experiment are as follows:
Initial conditions of the $2H_2 + O_2 + 7Ar$ system; temperature 298°K, pressure 0.1 atm.
Initial conditions of the high pressure H_2 side; temperature 298°K, pressure 5.0 atm.

The diaphragm which initially seperates the chemical system from the high pressure H_2 is assumed to be placed at a point 10.0 m from the downstream end (see Fig. 1). This is to give a visual idea on the shock propagation in the figures.

The discontinuities like shock front and contact surface are searched and determined, sensing the gradient change in temperature. To reduce the number of grids, an adaptive mesh system is used: The regions near shock front and contact discontinuity are discretised finely. The region between the shock and contact discontinuity is discretised with linearly increasing meshes. To conserve the number of grids a special technique is adopted. An imaginary marker is placed 30 grids before the contact discontinuity and the shock is allowed to propagate. Once the contact discontinuity crosses the imaginary marker, the solution process is temporarily stopped. The shock and the contact discontinuity are shifted back and placed in such a way that the contact discontinuity is 30 grids behind the imaginary marker described above. The grid is newly re-discretised and the flow properties are interpolated based on the new coordinates. The solution process is continued on the relocated system.

A set of elementary reactions describing the chemical reaction are given in Appendix A. The reaction contants of the respective reaction are also given. In the chemical calculation step, the time step $\triangle t$ is divided into 2 or more sub-steps where at each sub-step the reaction calculation is done implicitly. The conservation of species is tested at the end of all the sub-steps. If the species deficit is above the limit 0.001 percent, the number of sub-steps is increased during the next time step, where sometimes the total time step $\triangle t$ is divided into linearly increasing sub-steps, as shown in

$$\triangle t = \delta t + 2\delta t + \ldots + n\delta t\,.$$

The transient solution is presented at various time steps in Figs. 1 to 11. Since the plane discontinuity was not transversely disturbed, the shock propagates like a 1-D wave. The domain is divided into 200 grids in x direction and 30 grids in y direciton. The fine spacing in x direction is of the size 0.0005 m, while the y direction width is divided into an equal length 0.0005 m. The plain shock front was not disturbed by any irregularities, hence the shock ignites the mixture and propagates as a coupled wave. The distribution of flow properties is plotted along the length of the channel.

The velocity of the shock front and the velocity of the fluid near the shock front at various time steps are tabulated in Table 1. The values show that the velocity of the shock front varies between 1500 m/s and 1600 m/s. The fluid velocity near the shock front varies between 1080 m/s and 1140 m/s. Thus the shock front seems to have attained a steady-state propagation velocity with oscillation.

The plot of density, temperature and pressure clearly shows the propagation of a shock with combustion zone. The combustion zone is clearly visible after the time 110 μs (see the plots after N = 7000). From the figures after N = 7000, it may be observed that the combustion zone expands and contracts with respect to its width during propagation.

Table 1.

Time (μs)	Fluid velocity (m/s)	Shock velocity (m/s)
47	1094	1334
63	1130	1553
76	1130	1585
97	1120	1558
110	1102	1570
123	1105	1538
132	1103	1543
143	1096	1516
152	1098	1587
162	1083	1515
175	1084	1516
185	1094	1539
195	1105	1540
208	1115	1546
217	1120	1594
226	1128	1574
239	1134	1575
250	1133	1545
260	1125	1605
270	1108	1553

The program written in FORTRAN 77 is fully vectorised and run on a Fujitsu VP-200 machine. The solution time on average is 25 μs for a node per iteration, if chemical calculations are done in 2 sub-steps.

6. Conclusions

The present form of a time-split algorithm, with explicit solution of convective part and implicit solution of reaction part, seems to produce good results for reactive flows. The initiation and propagation of an undisturbed plane two-dimensional shock wave with a combustion front in a $2H_2 + O_2 + 7Ar$ system is numerically simulated using the present algorithm.

The velocity of shock front and the fluid velocity near the shock front are presented to show almost steady-state propagation of the shock front accompanied by a combustion front. The transient results on various flow properties are presented for visualisation.

The results show that the shock-initiated combustion travels like a shock wave accompanied by a combustion front, i.e. a detonation. As it progapates, the combustion zone behind the shock front expands and contracts with respect to its width; longitudinal oscillation.

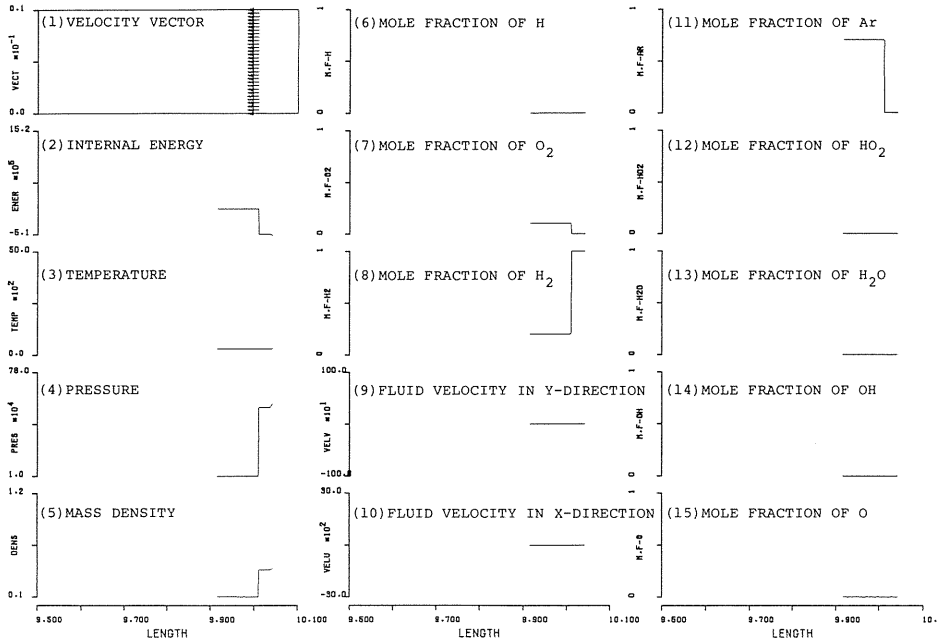

Fig. 1. At Time Step N = 0: Distribution of Various Physical Quantities along X-Direction.

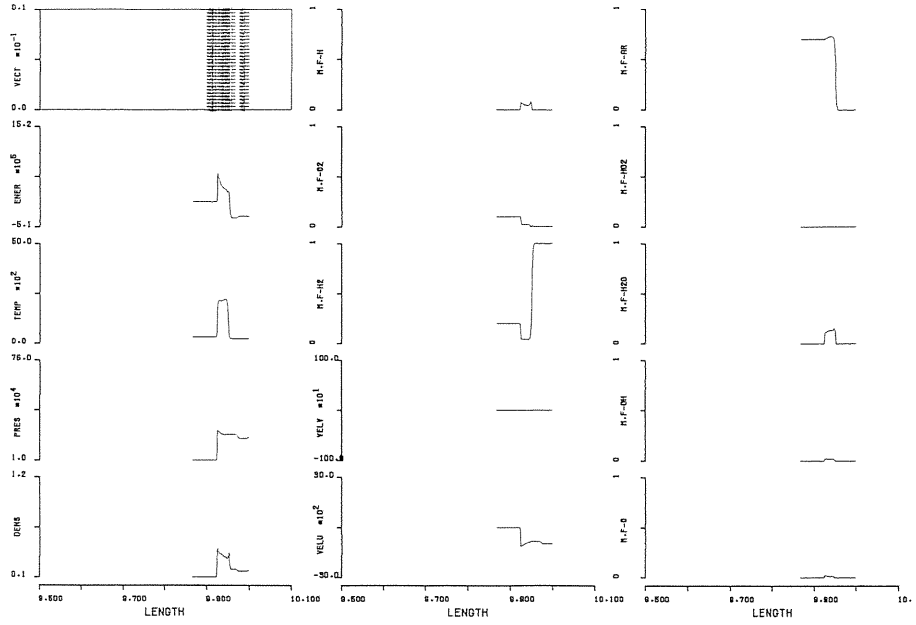

Fig. 2. At Time Step N = 2000.

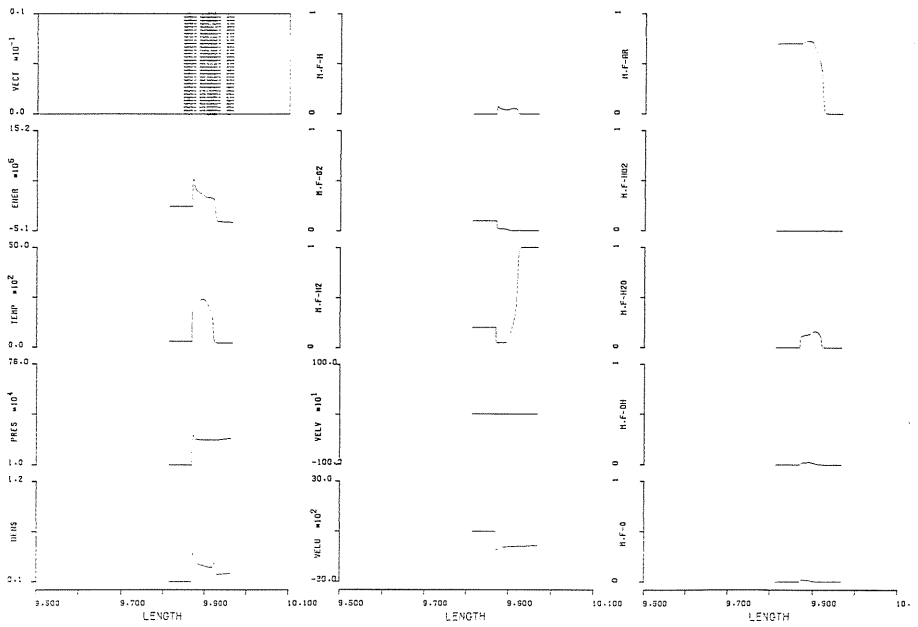

Fig. 3. At Time Step N = 5000.

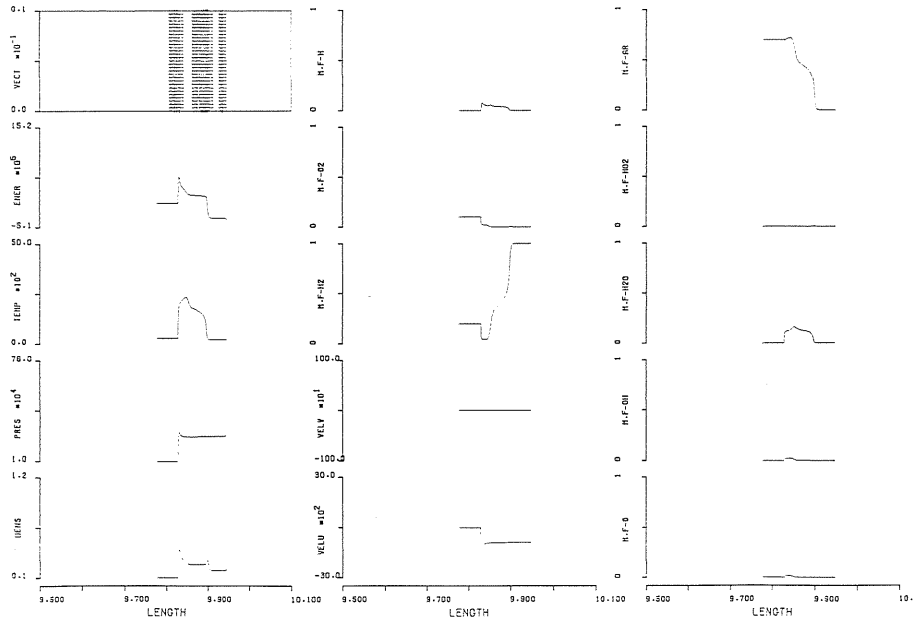

Fig. 4. At Time Step N = 7000.

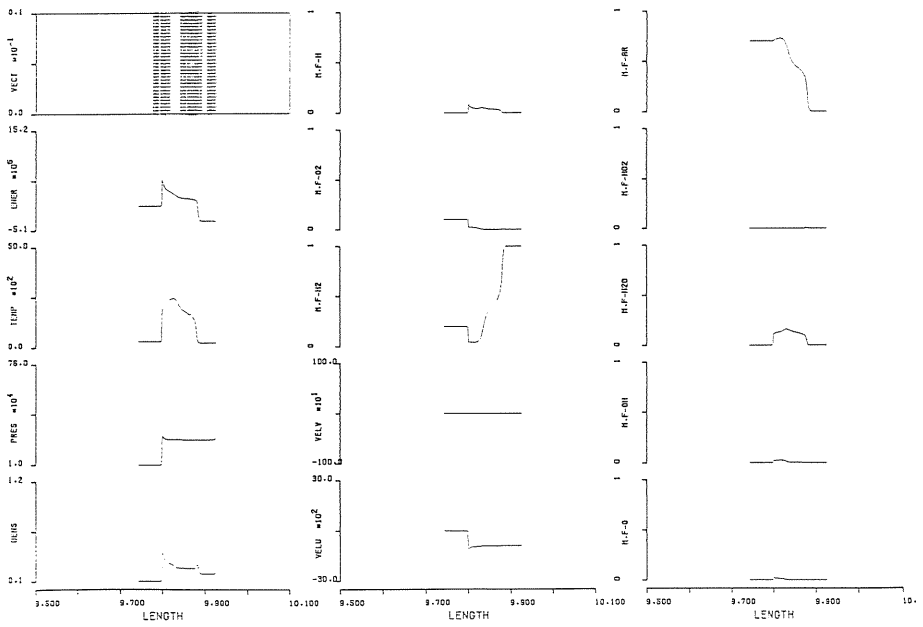

Fig. 5. At Time Step N = 9000.

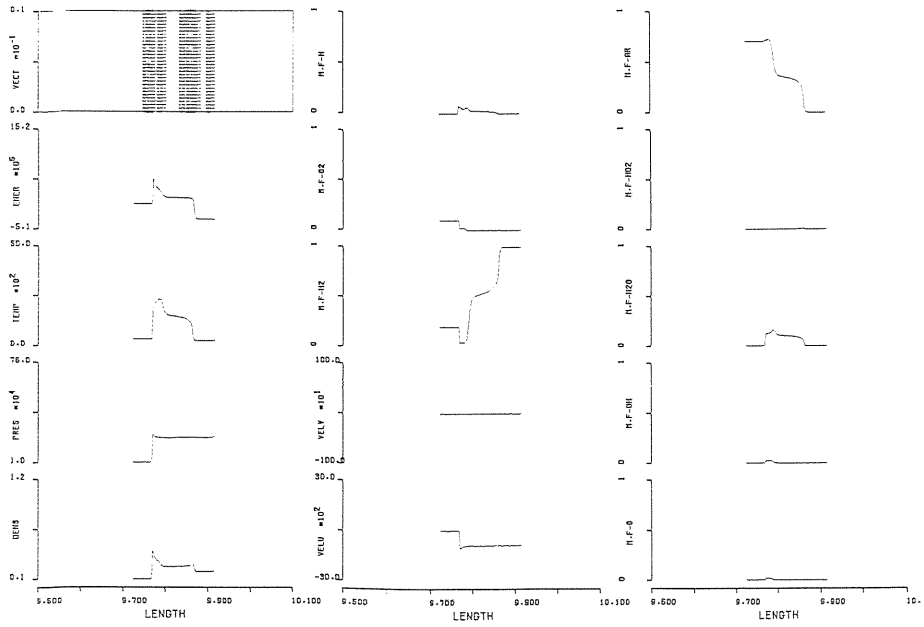

Fig. 6. At Time Step N = 11000.

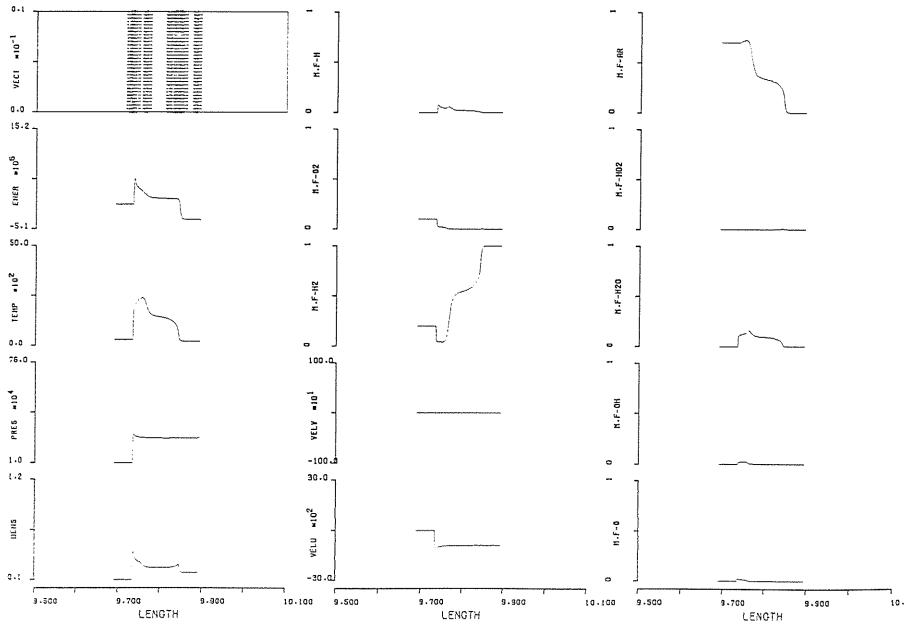

Fig. 7. At Time Step N = 13000.

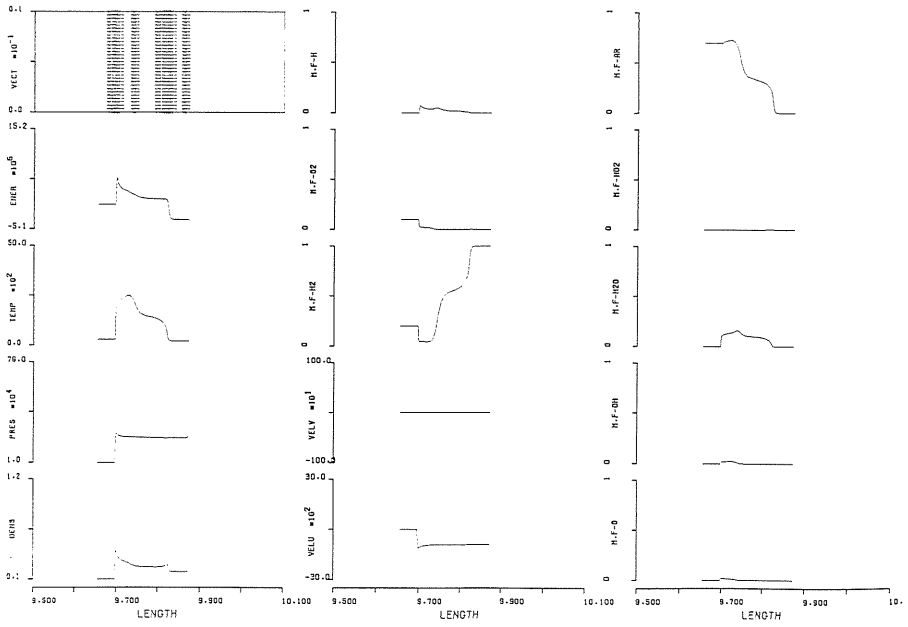

Fig. 8. At Time Step N = 15000.

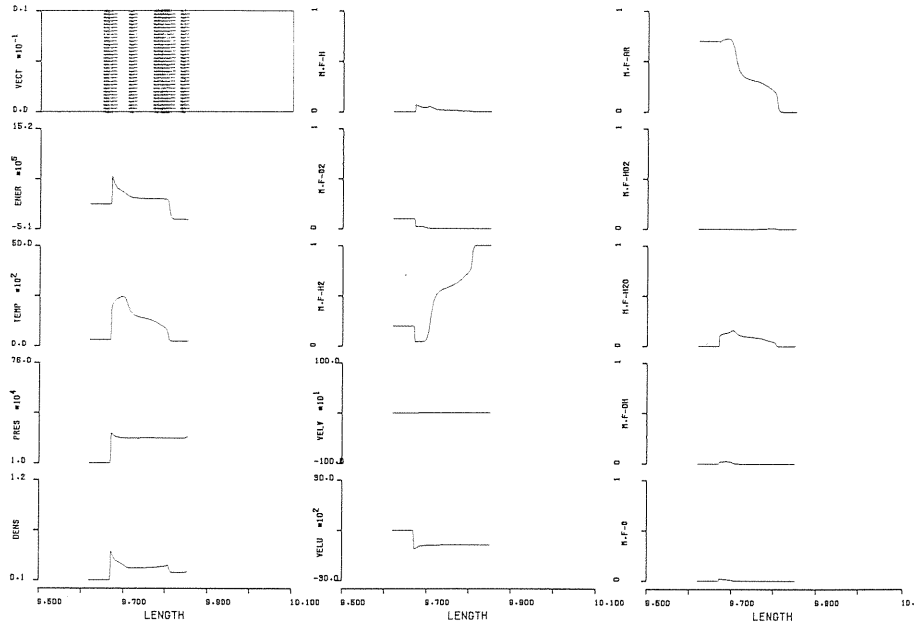

Fig. 9. At Time Step N = 17000.

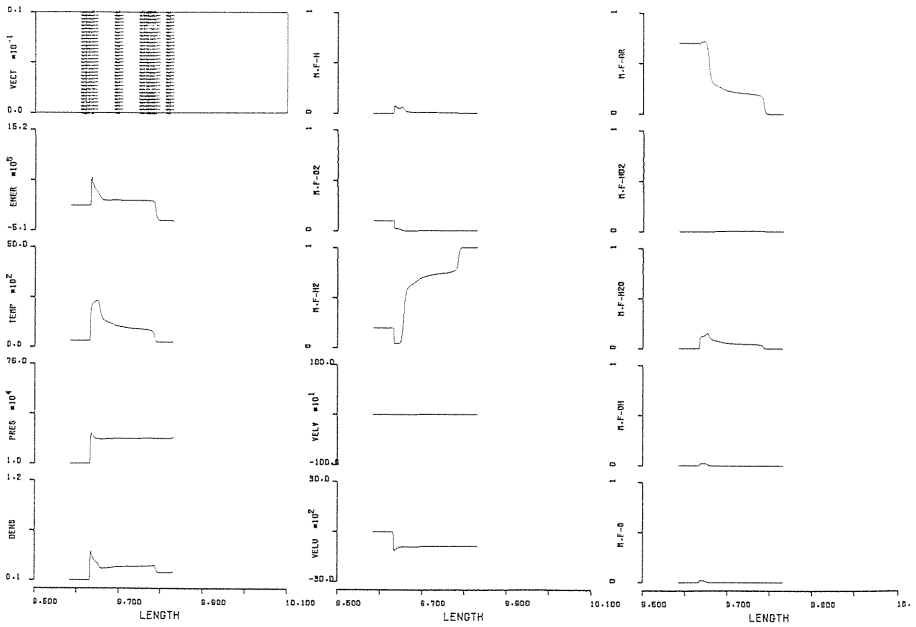

Fig. 10. At Time Step N = 19000.

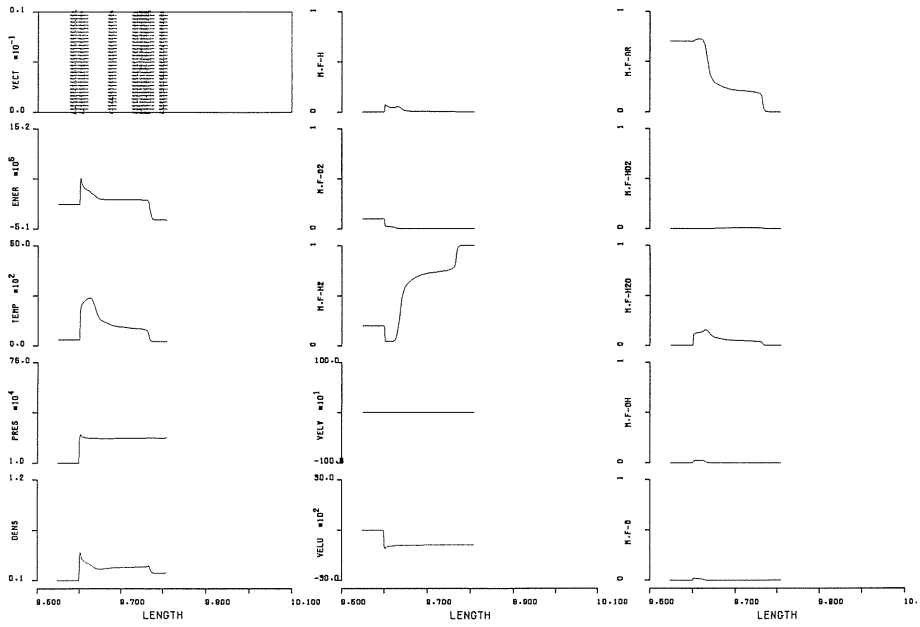

Fig. 11. At Time Step N = 21000.

7. References

1) A. Harten, Journal of Computational Physics. 49 (1983), 357.
2) H.C. Yee, NASA Technical Memorandum 89464, May 1985.
3) C.R. Chakravarthy and S. Osher, AIAA paper 85-0363, Jan. 1985.
4) J.L. Shinn and H.C. Yee, AIAA paper 87-1577, June 1987.
5) Yi-yun Wang and T. Fujiwara, AIAA paper 88-0478, Jan. 1988.
6) K.V. Reddy and T. Fujiwara, AIAA paper 88-2616, June 1988.
7) E. Oran, T. Young and J. Boris, 17th Symposium on Combustion The Combustion Institute, 1978, page 43.
8) Y. Wada, S. Ogawa and T. Ishiguro, AIAA paper 89-0202, Jan. 1989.
9) J.P. Drummond and M.Y. Hussaini, AIAA paper 87-1325, June 1987.
10) H. Lomax and H.E. Bailey, NASA Report TN D-4109.
11) R.J. Kee, J.A. Miller and T.H. Jefferson, CHEMKIN Report SAN80-8003 (1980).

8. Appendix

8. 1. A

The reactions describing the combustion process[9] are given below:

(R_1) $H_2 + O_2 = 2OH$

(R_2) $H + O_2 = \mathrm{OH} + \mathrm{O}$

(R_3) $OH + H_2 = H_2O + \mathrm{H}$

(R_4) $O + H_2 = \mathrm{OH} + \mathrm{H}$

(R_5) $2\mathrm{OH} = H_2O + \mathrm{O}$

(R_6) $\mathrm{H} + \mathrm{OH} + \mathrm{M} = H_2O + \mathrm{M}$

(R_7) $2\mathrm{H} + \mathrm{M} = H_2 + \mathrm{M}$

(R_8) $\mathrm{H} + O_2 = HO_2 + \mathrm{M}$

(R_9) $HO_2 + \mathrm{OH} = H_2O + O_2$

Constants in reaction rate:

Reaction	A_r	N_r	E_{ar}
R_1	$0.170 * 10^{14}$	0.0	48150
R_2	$0.142 * 10^{15}$	0.0	16400
R_3	$0.316 * 10^{8}$	1.8	3030
R_4	$0.207 * 10^{15}$	0.0	13750
R_5	$0.550 * 10^{14}$	0.0	7000
R_6	$0.221 * 10^{23}$	−2.0	0
R_7	$0.653 * 10^{18}$	−1.0	0
R_8	$0.320 * 10^{19}$	−1.0	0
R_9	$0.500 * 10^{14}$	0.0	1000

A_r (cm-mole-sec-K), E_{ar} (cal/mole).

8. 2. B

Coefficients for the polynomial of equilibrium constant K_{pi} (atm):

Species	d_{i1}	d_{i2}	d_{i3}	d_{i4}	d_{i5}
H	3.24199	−12.30420	0.56487	−0.17065	0.01983
O	3.54434	−13.56711	0.28589	−0.08002	0.00926
OH	0.67062	−1.75061	−0.23165	0.07491	−0.00875
H_2O	−3.10067	13.43635	−0.34220	0.07442	−0.00701
HO_2	−2.68084	−0.69023	−0.16401	0.03990	−0.00446
H_2	0.0	0.0	0.0	0.0	0.0
O_2	0.0	0.0	0.0	0.0	0.0
Ar	0.0	0.0	0.0	0.0	0.0

8. 3. C

Coefficients for the polynomial of enthalpy h_i (cal/g):

Species	b_{i0}	b_{i1}	b_{i2}	b_{i3}	b_{i4}	b_{i5}
H_2	−1043.636	3563.011	−283.171	276.550	−66.742	5.615
O_2	−60.373	185.385	63.308	−23.132	4.746	−0.382
H	50217.816	4925.994	3.288	−1.776	0.434	−0.039
O	3625.713	329.194	−15.772	6.633	−1.373	0.117
OH	431.639	418.362	−24.125	30.361	−7.984	0.703
H_2O	−3328.269	383.602	76.473	11.309	−6.253	0.656
HO_2	84.300	191.756	121.429	−38.088	6.445	−0.449
Ar	−38.001	127.550	0.000	0.000	0.000	0.000